Covert quantum communication over optical channels

Evan J.D. Anderson, 1,* Christopher K. Eyre, 2 , Isabel M. Dailey 3 , and Boulat A. Bash 1,3

Abstract: We explore the problem of covertly communicating qubits over the lossy thermalnoise bosonic channel, which is a quantum-mechanical model of many practical channels, including optical. Covert communication ensures that an adversary is unable to detect the presence of transmissions, which are concealed in channel noise. We investigate an achievable lower bound on quantum covert communication using photonic dual-rail qubits. This encoding has practical significance, as it has been proposed for long-range repeater-based quantum communication over optical channels.

Covert, or low probability of detection/intercept (LPD/LPI) communication renders adversaries unaware of the presence of transmission between two or more parties. The last decade saw much exploration of the fundamental limits of covert communication over classical channels, with [1–4] leading to many follow-on works. However, the physics which underpins these channels is quantum. This was taken into account in recent work on covert classical-quantum channels [5–9]. For all these channels, covert communication is fundamentally governed by the *square root law* (SRL) which limits communication that is both covert and reliable to $\propto \sqrt{n}$ bits over n channel uses. In this paper, we extend these results to quantum covert communication over lossy thermal-noise bosonic channels. Such channels model optical fiber, and free space communication in the optical, microwave, and radiofrequency regimes. Here, we study quantum covert communication over such a channel utilizing dual-rail photonic qubits.

Dual-rail qubits have been proposed to transmit quantum information over long-range repeater-based quantum networks [10–12]. The quantum-optical channels in these networks are modeled by lossy thermal-noise bosonic channels. Unlike the previous results that focused largely on quantum key distribution (QKD) [13–16], here we take a direct approach and use dual-rail encoding to address quantum covert communication over these channels. Specifically, we adapt the analysis from covert classical-quantum channels [5–9]. We believe that this approach extends naturally to other quantum encodings and channels. Analogous to the \sqrt{n} scaling for bits in the classical-classical and classical-quantum channels, we find achievability of the SRL where one can send at least $\propto \sqrt{n}$ covert qubits with the dual-rail encoding.

The remainder of this paper is organized as follows: in Section 1 we provide the mathematical preliminaries as well as the system and channel models. In Section 2 we describe the mathematical formalism underpinning covert communication and provide our results. Finally, we wrap up in Section 3 with a discussion of our results and future research.

1. Preliminaries

1.1. Dual-rail Qubits

The dual-rail qubit is a well-known encoding of qubits into single photons in linear-optical quantum computing [17] and quantum communication [10]. The dual-rail encoding is represented by the presence or absence of a single photon in two optical modes. The logical states are $|0\rangle_L = |01\rangle$ and $|1\rangle_L = |10\rangle$. The general logical qubit state $|\psi\rangle$ is then a superposition of the two logical states: $|\psi\rangle = \alpha|0\rangle_L + \beta|1\rangle_L = \alpha|01\rangle + \beta|10\rangle$ and $\hat{\rho}_{\alpha,\beta} = |\psi\rangle\langle\psi|$ is the state's density

¹Wyant College of Optical Sciences, University of Arizona, Tucson, AZ 85721, USA

²Department of Mathematics, Brigham Young University, Provo, UT 84602, USA

³Department of Electrical and Computer Engineering, University of Arizona, Tucson, AZ 85721, USA *ejdanderson@arizona.edu

operator with $\alpha, \beta \in \mathbb{C}$ normalized such that $|\alpha|^2 + |\beta|^2 = 1$.

1.2. System and Channel Model

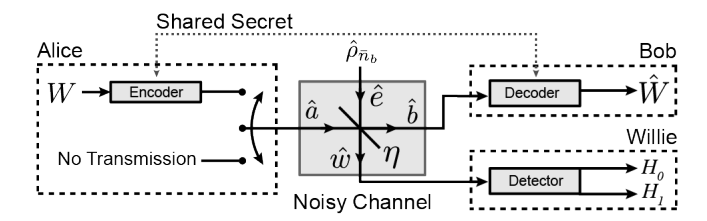


Fig. 1. Covert quantum communication model. Alice encodes a quantum message $|m\rangle$ and decides to transmit or not. The noisy channel is modeled by a beamsplitter with transmittance η . Annihilation operators \hat{a}, \hat{e} label Alice's and the environment's input modes, while \hat{b}, \hat{w} label Bob's and Willie's output modes. The environment acts on each mode independently, and hence the noisy channel block is applied 2n times. The environment is in a zero-mean thermal state $\hat{\rho}_{\bar{n}_b}$. Bob and Alice pre-share a secret, which they use to encode and decode quantum messages, while Willie attempts to detect their transmission.

Alice employs blocks of length n to encode each covert quantum message $|m\rangle$ using dual-rail qubits described in Section 1.1 and vacuum states $|00\rangle\langle00|$. Thus, she employs a total of 2n optical modes. Utilizing the pre-shared secret as described in Section 2, she modulates her transmission between sending a dual-rail qubit or not through the noisy channel, as detailed in Fig. 1. When Alice does not transmit, the input state to the channel is vacuum, $|00\rangle\langle00|$. The noisy channel acts on each mode independently, and Bob decodes the received state utilizing the shared secret to obtain an estimate $|\tilde{m}\rangle$ of the message. In the remainder of the paper, n uses of the channel employ a dual-rail qubit or the two-mode vacuum state $|00\rangle\langle00|$ on each use.

The noisy channel in Fig. 1 is modeled as a beamsplitter with transmittance $\eta \in [0, 1]$ and has the following input-output modal relationships:

$$\hat{b} = \sqrt{\eta}\hat{a} + \sqrt{1 - \eta}\hat{e} \text{ and } \hat{w} = \sqrt{1 - \eta}\hat{a} - \sqrt{\eta}\hat{e}, \tag{1}$$

where \hat{a} , \hat{e} , \hat{b} , and \hat{w} are the modal annihilation operators of Alice, the environment, Bob, and an adversary named Willie respectively. To model the lossy thermal-noise bosonic channel, the input state of mode \hat{e} is $\hat{\rho}_{\bar{n}_b}$, a zero-mean thermal state with mean photon number \bar{n}_b and expressed by the following sum over the diagonal elements in the Fock (photon number) basis $|k\rangle$:

$$\hat{\rho}_{\bar{n}_b} \equiv \sum_{k=0}^{\infty} t_k(\bar{n}_b) |k\rangle\langle k|, \tag{2}$$

where

$$t_k(\bar{n}_b) = \frac{\bar{n}_b^k}{(1 + \bar{n}_b)^{k+1}}. (3)$$

1.3. Entanglement Breaking Channel

An entanglement breaking channel is one that breaks entanglement between input quantum states at the output of the channel. Entanglement is broken in our Gaussian channel under the condition $\bar{n} > \kappa$ [18] where \bar{n} is the mean photon number of the thermal-noise at the output of the channel

and κ is the transmissivity of the input signal. In the following analysis, we assume that the Alice-to-Willie channel is naturally entanglement-breaking, corresponding to $\eta \bar{n}_b > 1 - \eta$, as is typical in optical communication systems. It is unknown whether the channel to the adversary must be entanglement-breaking for covert quantum communication, and is a subject of ongoing investigation. However, if the physical channel does not break entanglement, Alice may introduce additional loss and noise after encoding to ensure entanglement is broken leading to the following two lemmas:

Lemma 1. Entanglement can be broken in the Alice-to-Willie channel using an additional beamsplitter of transmissivity τ that mixes her signal with vacuum, yielding the entanglement breaking condition of $\eta \bar{n}_b > (1 - \eta)(1 - 2\tau)$.

Lemma 2. Entanglement can be broken in the Alice-to-Willie channel using a quantum-limited amplifier with gain coefficient $G = 2(1 - \eta)/(2(1 - \eta) - \eta \bar{n}_b')$ followed by a beamsplitter with transmissivity $\tau = 1/G$ and vacuum input on the second port. This yields the entanglement breaking condition of $\eta(\bar{n}_b + \bar{n}_b') > (1 - \eta)$.

Proofs of Lemma 1 and Lemma 2 can be found in Appendix B. In both cases, this reduces the number of qubits transmitted reliably and covertly by a constant factor. The SRL scaling is unaffected.

2. Covert Communication

Denote $\hat{\rho}_0^{W^n}$ and $\hat{\rho}_1^{W^n}$ as the respective states Willie observes when Alice is quiet or transmitting. Since two-mode vacuum $|00\rangle\langle00|$ is input when Alice is quiet, $\hat{\rho}_0^{W^n} = \left(\hat{\rho}_0^W\right)^{\otimes n}$, where $\hat{\rho}_0^W = \hat{\rho}_{\eta\bar{n}_b}\otimes\hat{\rho}_{\eta\bar{n}_b}$ is a two-mode thermal product state [19]. Willie desires to determine if Alice and Bob are communicating; ergo, in n uses of the two-mode bosonic channel, he tries to distinguish between $\hat{\rho}_1^{W^n}$ and $\left(\hat{\rho}_0^W\right)^{\otimes n}$. The null and alternate hypotheses H_0 and H_1 correspond to Alice being quiet and transmitting, respectively. Willie collects all the photons that do not reach Bob, as shown in Fig. 1.

Willie can make two types of errors: a false alarm, where he decides that Alice is transmitting when she is not (choosing H_1 when H_0 is true), and a missed detection, where he decides that Alice is not transmitting when she is (choosing H_0 when H_1 is true). As is customary in the literature, we assume equal prior probabilities for the hypotheses $P(H_0) = P(H_1) = \frac{1}{2}$. Thus, Willie's probability of error is: $P_e = \frac{P(H_0|H_1) + P(H_1|H_0)}{2}$.

Willie guessing randomly yields an ineffective detector with $P_e = \frac{1}{2}$. Hence, Alice's goal is to transmit so that P_e is as close to $\frac{1}{2}$ as possible. Formally, we call any system covert if, for large enough n and $\delta > 0$, $P_e \ge \frac{1}{2} - \delta$. With access to a quantum-optimal receiver, Willie can achieve minimal $P_e = \frac{1}{2} - \frac{1}{4} \left\| \hat{\rho}_1^{W^n} - \left(\hat{\rho}_0^W \right)^{\otimes n} \right\|_1$ [20, Ch. 9.1.4], where $\|\hat{A}\|_1$ is the trace norm of

$$\hat{A}$$
 [20, Def. 9.1.1]. This implies our system is covert if $\frac{1}{4} \left\| \hat{\rho}_1^{W^n} - \left(\hat{\rho}_0^W \right)^{\otimes n} \right\|_1 \le \delta$.

The trace distance is often mathematically unwieldy and the quantum relative entropy (QRE), $D(\hat{\rho}||\hat{\sigma}) = \text{tr}[\hat{\rho}\log\hat{\rho} - \hat{\rho}\log\hat{\sigma}]$, is commonly employed in covertness analysis [5–7] due to its additivity over product states. Indeed, the QRE upper bounds the trace distance via the quantum Pinsker's inequality [20, Th. 11.9.1],

$$\left\|\hat{\rho}_1^{W^n} - \left(\hat{\rho}_0^W\right)^{\otimes n}\right\|_1 \le \sqrt{2\ln(2)D\left(\hat{\rho}_1^{W^n} || \left(\hat{\rho}_0^W\right)^{\otimes n}\right)}.\tag{4}$$

The quantum covert communication system is constructed prior to transmission in two stages. First, Alice and Bob randomly select the dual-rail systems that they will use via n flips of a biased coin, with probability of heads q to be determined later. If the i^{th} flip is heads, then the i^{th} dual-rail system is selected. Second, a random coding technique described in [20, Section 23.3 and 24.4] is used to construct an encoder at Alice and a corresponding decoder at Bob that will only employ the systems selected in the first stage. As in the classical analogue [2], the chosen dual-rail systems and the random code instantiation are kept secret, while the procedure used as well as the time of transmission are known to Willie. Since the code is unknown to Willie and his channel from Alice is entanglement-breaking, the state he observes is a classical superposition of product states given by

$$\hat{\rho}_1^{W^n} = \sum_{\substack{\vec{k} \in \mathcal{K} \\ |m\rangle \in \mathcal{M}}} p\left(\vec{k}, |m\rangle\right) \bigotimes_{i=1}^n \hat{\rho}_{1,i}^W, \tag{5}$$

where \mathcal{M} is the set of messages, \mathcal{K} is a sufficiently large randomizing set of n-symbol vectors \vec{k} (see [20, Section 23.3 and 24.4]), and $\sum_{\substack{\vec{k} \in \mathcal{K} \\ |m\rangle \in \mathcal{M}}} p\left(\vec{k}, |m\rangle\right) = 1$. Furthermore,

$$\hat{\rho}_{1,i}^{W} = (1 - q)\hat{\rho}_{0}^{W} + q\hat{\rho}_{\alpha_{i},\beta_{i}}^{W},\tag{6}$$

where $\alpha_i, \beta_i \in X$ such that $|\alpha_i|^2 + |\beta_i|^2 = 1$, and X is a fixed set of complex amplitudes used in the random code. Then, substitution of (5) into the QRE yields the following upper bound on the QRE between states $\hat{\rho}_1^{W^n}$ and $(\hat{\rho}_0^W)^{\otimes n}$:

$$\left(\hat{\rho}_{1}^{W^{n}} \| \left(\hat{\rho}_{0}^{W}\right)^{\otimes n}\right) \leq \sum_{\substack{\vec{k} \in \mathcal{K} \\ |m\rangle \in M}} p\left(\vec{k}, |m\rangle\right) D\left(\bigotimes_{i=1}^{n} \hat{\rho}_{1,i}^{W} \| \left(\hat{\rho}_{0}^{W}\right)^{\otimes n}\right) \tag{7}$$

$$= \sum_{\substack{\vec{k} \in \mathcal{K} \\ |m\rangle \in M}} p\left(\vec{k}, |m\rangle\right) \sum_{i=1}^{n} D\left(\hat{\rho}_{1,i}^{W} \| \left(\hat{\rho}_{0}^{W}\right)^{\otimes n}\right) \tag{8}$$

$$\leq \sum_{\substack{\vec{k} \in \mathcal{K} \\ |m\rangle \in M}} p\left(\vec{k}, |m\rangle\right) q^2 \sum_{i=1}^n D_{\chi^2}\left(\hat{\rho}_{\alpha_i, \beta_i}^W \|\hat{\rho}_0^W\right),\tag{9}$$

where (7) and (8) follow from the convexity [20, Corollary 11.9.2] and additivity [20, Ex. 11.8.7] properties of the QRE. Lastly, (9) is by [9, Lemma 1], where the quantum χ^2 -divergence [21] between two states $\hat{\rho}$ and $\hat{\sigma}$ is:

$$D_{\chi^2}(\hat{\rho}||\hat{\sigma}) = \text{tr}\left[(\hat{\rho} - \hat{\sigma})^2 \hat{\sigma}^{-1}\right] = \text{tr}[\hat{\rho}^2 \hat{\sigma}^{-1}] - 1, \tag{10}$$

with the second equality due to the cyclic property of the trace and the fact that the trace of a quantum state is unity. The following theorem yields an expression for $D_{\chi^2}\left(\hat{\rho}^W_{\alpha_i,\beta_i}\|\hat{\rho}^W_0\right)$:

Theorem 1. When the Alice-to-Willie channel is entanglement breaking, the χ^2 -divergence between the states $\hat{\rho}_{\alpha,\beta}^W$ and $\hat{\rho}_0^W$, for arbitrary $\alpha,\beta\in\mathbb{C}$ such that $|\alpha|^2+|\beta|^2=1$, is

$$D_{\chi^2}(\hat{\rho}_{\alpha,\beta}^W||\hat{\rho}_0^W) = \frac{(1-\eta)^2}{\eta \bar{n}_b (1+\eta \bar{n}_b)}.$$
 (11)

Proof. The state $\hat{\rho}_0^W$ is the result of mixing a vacuum and zero-mean thermal state with mean photon number \bar{n}_b and has a well-known solution, $\hat{\rho}_0^W = \hat{\rho}_{\eta\bar{n}_b}$ [19]. Determining $\hat{\rho}_{\alpha,\beta}^W$ is more complicated. First, we find its density operator representation. The anti-normally ordered characteristic function of state a $\hat{\rho}$ is:

$$\chi_A^{\hat{\rho}}(\zeta, \zeta^*) = \operatorname{tr}\left[\hat{\rho}e^{-\zeta^*\hat{a}}e^{\zeta\hat{a}^{\dagger}}\right],\tag{12}$$

where $\zeta \in \mathbb{C}$ and $\hat{a}, \hat{a}^{\dagger}$ are modal annihilation and creation operators [19]. The anti-normally ordered characteristic function completely defines a quantum state.

For brevity, denote $\chi_A^{\hat{\rho}_{\alpha,\beta}^W}(\zeta^*,\zeta)$ by $\chi_A^{\hat{\rho}_{\alpha,\beta}^W}$. Using the modal relationship of the beamsplitter (1), we have

$$\chi_A^{\hat{\rho}_{\alpha\beta}^W} = \chi_A^{\hat{\rho}_e} \left(\sqrt{\eta} \zeta^*, \sqrt{\eta} \zeta, \right) \chi_A^{\hat{\rho}_a} \left(\sqrt{1 - \eta} \zeta^*, \sqrt{1 - \eta} \zeta \right) \tag{13}$$

where $\chi_A^{\hat{\rho}_e}$ and $\chi_A^{\hat{\rho}_a}$ are the characteristic functions for the thermal state and Alice's dual-rail qubit. The expression for $\chi_A^{\hat{\rho}_e}$ is well known [22, Section 7.4.3.2], while $\chi_A^{\hat{\rho}_a}$ is derived by substituting $\hat{\rho}_{\alpha,\beta}$ into (12) and Taylor-expanding the exponentials, yielding:

$$\chi_A^{\hat{\rho}_{\alpha,\beta}^W} = e^{-(1+\eta\bar{n}_b)|\zeta|^2} \left[|\alpha|^2 + |\beta|^2 (1-\eta)|\zeta|^2 - \alpha\beta^* \sqrt{1-\eta}\zeta - \alpha^*\beta\sqrt{1-\eta}\zeta^*. \right]$$
(14)

A state $\hat{\rho}$ and its characteristic function are related via the operator Fourier transform [19]:

$$\hat{\rho}_{\alpha,\beta}^{W} = \iint \frac{d^{2}\zeta_{1}}{\pi} \frac{d^{2}\zeta_{2}}{\pi} \chi_{A}^{\hat{\rho}_{\alpha,\beta}^{W}} e^{\zeta_{2}\hat{w}_{2}^{\dagger}} e^{\zeta_{1}\hat{w}_{1}^{\dagger}} e^{-\zeta_{1}^{*}\hat{w}_{1}} e^{-\zeta_{2}^{*}\hat{w}_{2}}, \tag{15}$$

where the integrals are over the entire complex plane for ζ_1 and ζ_2 . Furthermore, given the Fock number basis, the density operator elements $p_{f,g,f',g'}$ are found as follows:

$$p_{f,g,f',g'} = \langle fg | \hat{\rho}_{\alpha,\beta}^W | f'g' \rangle \quad \forall f,g,f',g' \in \mathbb{N}_0.$$
 (16)

The integrals in (15) are evaluated in polar coordinates and with Taylor expansions of the exponentials that include annihilation and creation operators. Due to the orthogonality of Fock states for the $|\alpha|^2$ and $|\beta|^2$ contributions, the only terms that remain are when f=f' and g=g', which corresponds to the main diagonal of the density operator. The terms for the $\alpha\beta^*$ contribution are non-zero when f'=f+1 and g'=g-1, which originate from an off-by-one exponential in integration over the corresponding polar coordinates. The $\alpha^*\beta$ contributions follow similarly with the requirement f'=f-1 and g'=g+1. The Fourier transform in (15) thus yields the state:

$$\hat{\rho}_{\alpha,\beta}^{W} = \sum_{g=0}^{\infty} \sum_{f=0}^{\infty} |\alpha|^{2} \frac{(\eta \bar{n}_{b})^{f}}{(1+\eta \bar{n}_{b})^{f+1}} \left(\frac{(\eta \bar{n}_{b})^{g}}{(1+\eta \bar{n}_{b})^{g+1}} - \frac{(1-\eta)(\eta \bar{n}_{b}-g)(\eta \bar{n}_{b})^{g-1}}{(1+\eta \bar{n}_{b})^{g+2}} \right) |fg\rangle\langle fg|$$

$$+ |\beta|^{2} \frac{(\eta \bar{n}_{b})^{g}}{(1+\eta \bar{n}_{b})^{g+1}} \left(\frac{(\eta \bar{n}_{b})^{f}}{(1+\eta \bar{n}_{b})^{f+1}} - \frac{(1-\eta)(\eta \bar{n}_{b}-f)(\eta \bar{n}_{b})^{f-1}}{(1+\eta \bar{n}_{b})^{f+2}} \right) |fg\rangle\langle fg|$$

$$+ \frac{(1-eta)(\eta \bar{n}_{b})^{g+f-1}}{(1+\eta \bar{n}_{b})^{g+f+3}} \left(\alpha^{*}\beta\sqrt{f}\sqrt{g+1} |fg\rangle\langle f-1,g+1| \right)$$

$$+\alpha\beta^{*}\sqrt{g}\sqrt{f+1} |fg\rangle\langle f+1,g-1| \right)$$

$$(17)$$

$$\begin{split} \hat{\rho}^W_{\alpha,\beta} \text{ is a tri-diagonal matrix as it is defined by } |fg\rangle\langle fg|, |fg\rangle\langle f-1,g+1|, \text{ and } |fg\rangle\langle f+1,g-1| \\ \text{where the coefficients for the states involving } \langle f-1| \text{ and } \langle g-1| \text{ are 0 when } f=0 \text{ or } g=0. \\ \text{Calculating } (\hat{\rho}^W_{\alpha,\beta})^2 \text{ involves equating each diagonal to own matrix } \hat{A}, \hat{B}, \hat{C} \text{ and computing } \\ (\hat{\rho}^W_{\alpha,\beta})^2 = \left(\hat{A} + \hat{B} + \hat{C}\right)^2. \end{split}$$

Finally, recall that the density operator $\hat{\rho}_0^W$ describing the state received by Willie when Alice does not transmit is

$$\hat{\rho}_0^W = \sum_{f=0}^{\infty} \sum_{g=0}^{\infty} t_g(\eta \bar{n}_b) t_f(\eta \bar{n}_b) |fg\rangle \langle fg|, \tag{18}$$

where $t_f(\eta \bar{n}_b)$ and $t_g(\eta \bar{n}_b)$ are defined in (3). Since (18) is a diagonal operator, its inverse is also diagonal. Calculating $D_{\chi^2}(\hat{\rho}^W_{\alpha,\beta}||\hat{\rho}^W_0) = \mathrm{tr}[(\hat{\rho}^W_{\alpha,\beta})^2(\hat{\rho}^W_0)^{-1}] - 1$ thus reduces to multiplying the diagonal elements of $(\hat{\rho}^W_{\alpha,\beta})^2$ and $(\hat{\rho}^W_0)^{-1}$, and summing the results. This yields:

$$\operatorname{tr}[(\hat{\rho}_{\alpha,\beta}^{W})^{2}(\hat{\rho}_{0}^{W})^{-1}] = \frac{(1-\eta)^{2}}{\eta \bar{n}_{b}(1+\eta \bar{n}_{b})} + 1. \tag{19}$$

Subtracting 1 from (19) completes the proof.

Note: Since the Alice-to-Willie channel is entanglement-breaking, this proof may be simplified further and is an avenue we are currently exploring. A full proof with all mathematical steps is found in Appendix A.

Theorem 1 shows the independence of $D_{\chi^2}(\hat{\rho}^W_{\alpha,\beta}||\hat{\rho}^W_0)$ on Alice's state parameters α and β . Combining (4), (9), and the result of Theorem 1 yields

$$\frac{1}{4} \left\| \hat{\rho}_1^{W^n} - \left(\hat{\rho}_0^W \right)^{\otimes n} \right\|_1 \le \frac{q(1 - \eta)\sqrt{\ln(2)n}}{2\sqrt{2\eta\bar{n}_b}(1 + \eta\bar{n}_b)}.$$
 (20)

Therefore, the covertness requirement is maintained if $q \leq \frac{c_{\text{cov}}\delta}{\sqrt{n}}$, where the covertness constant is $c_{\text{cov}} \leq \frac{2\sqrt{2\eta\bar{n}_b(1+\eta\bar{n}_b)}}{\sqrt{\ln 2}(1-\eta)}$.

2.1. Reliability Analysis

Let M(n) be the number of qubits transmitted covertly in n channel uses. Then, $E[M(n)] = nqR \propto \sqrt{n}$, where R is the constant rate of reliable qubit transmission per channel use and $nq \propto \sqrt{n}$ is the expected number of these channel uses selected by Alice and Bob for transmission in the first stage of construction. We lower bound R as follows:

Theorem 2.
$$R \ge 1 - H(\vec{p})$$
, where $\vec{p} = (1 - \frac{3p}{4}, \frac{p}{4}, \frac{p}{4}, \frac{p}{4})$, $p = \frac{2(1-\eta)^2 \bar{n}_b (1+\bar{n}_b)}{\eta + 2(1-\eta)^2 \bar{n}_b (1+\bar{n}_b)}$, and $H(\vec{p}) = -\sum_{p_i \in \vec{p}} p_i \log(p_i)$.

Proof (Sketch). If Bob discards the received two-mode states that do not contain a single photon, the channel reduces to a depolarizing channel parameterized by p [23, Appendix B]. This is further represented as a Pauli channel with $p_I = 1 - \frac{3p}{4}$ and $p_X = p_Y = p_Z = \frac{p}{4}$ [20, Section 4.7.4]. The lemma follows from the fact that we employ the random codes from [20, Section 23.3 and 24.4] in construction and the hashing bound [20, Section 24.6.3].

We note that largest achievable R is given by the regularized coherent information [20, Th. 24.3.1], which is challenging to compute for many channels, including the depolarizing channel. Hence, we employ the hashing bound. However, we are also exploring better bounds.

3. Conclusion

We have lower-bounded the square root scaling factor c_{cov} for the dual-rail qubit encoding over the lossy thermal-noise bosonic channel, as well as provided a lower bound on the expected number E[M(n)] of qubits that are covertly and reliably transmissible over a bosonic channel. There are many avenues for future work. The framework provided in this manuscript may be applied to other qubit encodings and quantum channels. Our bound on c_{cov} looks similar to that for the classical-quantum covert communication in [6]. We believe that the proof in Theorem 1 can be further simplified using the entanglement-breaking condition of Alice-to-Willie channel. Our covertness scheme requires a substantial number of classical pre-shared secret bits; resolvability techniques from [3,9] should be adapted to reduce this burden. Indeed, practical codes enabling a physical realization of the protocol should be investigated (e.g., quantum Reed-Muller codes [24] achieve the quantum capacity of an erasure channel). Deriving the quantum covert capacity requires the development of the converse which is likely challenging. Indeed, even the non-covert quantum capacity of such a channel remains a difficult task due to the optimization over regularized coherent information [25] Finally, although we specifically address quantum communication rather than QKD, we expect our work to provide insight into the open questions in covert QKD [13–16].

References

- B. A. Bash, D. Goeckel, S. Guha, and D. Towsley, "Hiding information in noise: Fundamental limits of covert wireless communication," IEEE Commun. Mag. 53 (2015).
- B. A. Bash, D. Goeckel, and D. Towsley, "Limits of reliable communication with low probability of detection on AWGN channels," IEEE J. Sel. Areas Commun. 31, 1921–1930 (2013).
- M. R. Bloch, "Covert communication over noisy channels: A resolvability perspective," IEEE Trans. Inf. Theory 62, 2334–2354 (2016).
- L. Wang, G. W. Wornell, and L. Zheng, "Fundamental limits of communication with low probability of detection," IEEE Trans. Inf. Theory 62, 3493–3503 (2016).
- B. A. Bash, A. H. Gheorghe, M. Patel, et al., "Quantum-secure covert communication on bosonic channels," Nat. Commun. 6 (2015).
- M. S. Bullock, C. N. Gagatsos, S. Guha, and B. A. Bash, "Fundamental limits of quantum-secure covert communication over bosonic channels," IEEE J. Sel. Areas Commun. 38, 471–482 (2020).
- C. N. Gagatsos, M. S. Bullock, and B. A. Bash, "Covert capacity of bosonic channels," IEEE J. Sel. Areas Inf. Theory 1, 555–567 (2020).
- 8. A. Sheikholeslami, B. A. Bash, D. Towsley, *et al.*, "Covert communication over classical-quantum channels," in *Proc. IEEE Int. Symp. Inform. Theory (ISIT)*, (Barcelona, Spain, 2016).
- M. S. Bullock, A. Sheikholeslami, M. Tahmasbi, et al., "Covert Communication over Classical-Quantum Channels," arXiv:1601.06826v7 [quant-ph] (2023).
- S. Takeda, T. Mizuta, M. Fuwa, et al., "Deterministic quantum teleportation of photonic quantum bits by a hybrid technique," Nature 500, 315–318 (2013).
- S. Guha, H. Krovi, C. A. Fuchs, et al., "Rate-loss analysis of an efficient quantum repeater architecture," Phys. Rev. A 92, 022357 (2015).
- P. Dhara, D. Englund, and S. Guha, "Entangling quantum memories via heralded photonic bell measurement," arXiv:2303.03453 [quant-ph] (2023).
- 13. J. M. Arrazola and V. Scarani, "Covert Quantum Communication," Phys. Rev. Lett. 117, 250503 (2016).
- M. Tahmasbi and M. R. Bloch, "Framework for covert and secret key expansion over classical-quantum channels," Phys. Rev. A 99, 052329 (2019).
- M. Tahmasbi and M. R. Bloch, "Toward undetectable quantum key distribution over bosonic channels," IEEE J. Sel. Areas Inf. Theory 1, 585–598 (2020).
- M. Tahmasbi and M. R. Bloch, "Covert and secret key expansion over quantum channels under collective attacks," IEEE Trans. Inf. Theory 66, 7113–7131 (2020).
- 17. E. Knill, R. Laflamme, and G. J. Milburn, "A scheme for efficient quantum computation with linear optics," Nature 409, 46–52 (2001).
- 18. A. S. Holevo, "Entanglement-breaking channels in infinite dimensions," Probl. Inf. Transm. 44, 171–184 (2008).
- 19. C. Weedbrook, S. Pirandola, R. García-Patrón, *et al.*, "Gaussian quantum information," Rev. Mod. Phys. **84**, 621–669
- 20. M. Wilde, *Quantum Information Theory* (Cambridge University Press, 2016), 2nd ed.
- K. Temme, M. J. Kastoryano, M. Ruskai, et al., "The \(\chi^2\)-divergence and mixing times of quantum Markov processes,"
 J. Math. Phys. 51, 122201 (2010).

- 22. M. Orszag, Quantum Optics (Springer, Berlin, Germany, 2016), 3rd ed.
- S. P. Kish, P. Gleeson, P. K. Lam, and S. M. Assad, "Comparison of discrete variable and continuous variable quantum key distribution protocols with phase noise in the thermal-loss channel," arXiv:2206.13724 [quant-ph] (2023).
- S. Kumar, R. Calderbank, and H. D. Pfister, "Reed-muller codes achieve capacity on the quantum erasure channel," in 2016 Proc. IEEE Int. Symp. Inform. Theory, (2016), pp. 1750–1754.
- S. Khatri, K. Sharma, and M. M. Wilde, "Information-theoretic aspects of the generalized amplitude-damping channel," Phys. Rev. A 102, 012401 (2020).

Funding. This work was supported by the National Science Foundation under Grants No. CCF-2006679 and EEC-1941583.

Appendix A. Proof of Theorem 1

The proof of Theorem 1 is shown in the following way: we first derive the state at Willie when Alice chooses to transmit, then we compute the quantum χ^2 -divergence between that state and the state received by Willie when Alice is not transmitting.

A.1. State at Willie

When Alice does not transmit, Willie observes a two-mode attenuated thermal state of

$$\hat{\rho}_0^W = \sum_{n=0}^{\infty} \sum_{m=0}^{\infty} \frac{\eta N^n}{(\eta N + 1)^{n+1}} \frac{\eta N^m}{(\eta N + 1)^{m+1}} |nm\rangle \langle nm| \tag{A.1}$$

where N is the thermal mean-photon number of the environment state, η is the transmissivity of the channel and $|nm\rangle$ is the Fock basis. When Alice chooses to transmit, her input state to the beamsplitter is given by a dual-rail qubit. Hence, we consider input states for Alice $\hat{\rho}_a$ and the thermal environment $\hat{\rho}_e$ into the channel of Fig. 1 where

$$\hat{\rho}_a = |\alpha|^2 |01\rangle\langle 01| + \alpha\beta^* |01\rangle\langle 10| + \alpha^*\beta |10\rangle\langle 01| + |\beta|^2 |10\rangle\langle 10| \tag{A.2}$$

$$\hat{\rho}_e = \sum_{n=0}^{\infty} \sum_{m=0}^{\infty} \frac{N^n}{(N+1)^{n+1}} \frac{N^m}{(N+1)^{m+1}} |nm\rangle \langle nm|$$
(A.3)

The relationship between modal annihilation (and creation) operators at the output mode labeled \hat{w} in Fig. 1 is given by

$$\hat{w} = \sqrt{1 - \eta} \hat{a} - \sqrt{\eta} \hat{e}. \tag{A.4}$$

Let us now find the Fock representation of the output state $\hat{\rho}_w$ of Warden when Alice transmits a qubit. We utilize the anti-normally ordered characteristic function for $\hat{\rho}_w$:

$$\chi_A^{\hat{\rho}_W} \left(\zeta_1^*, \zeta_1, \zeta_2^*, \zeta_2 \right) = \operatorname{tr}(\hat{\rho}_W e^{-\zeta_1^* \hat{w}_1} e^{\zeta_1 \hat{w}_1^{\dagger}} e^{-\zeta_2^* \hat{w}_2} e^{\zeta_2 \hat{w}_2^{\dagger}}). \tag{A.5}$$

Furthermore, let $\langle \cdot \rangle_x$ denote the expected value of an operator when applied to the state $\hat{\rho}_x$ for $x \in \{a, w, e\}$, we have

$$\chi_A^{\hat{\rho}_W}\left(\zeta_1^*, \zeta_1, \zeta_2^*, \zeta_2\right) \tag{A.6}$$

$$= \langle e^{-\zeta_1^* \hat{w}_1} e^{\zeta_1 \hat{w}_1^{\dagger}} e^{-\zeta_2^* \hat{w}_2} e^{\zeta_2 \hat{w}_2^{\dagger}} \rangle_w \tag{A.7}$$

$$= \langle e^{-\zeta_1^* (\sqrt{1-\eta} \hat{a}_1 - \sqrt{\eta} \hat{e}_1)} e^{\zeta_1 (\sqrt{1-\eta} \hat{a}_1^{\dagger} - \sqrt{\eta} \hat{e}_1^{\dagger})} e^{-\zeta_2^* (\sqrt{1-\eta} \hat{a}_2 - \sqrt{\eta} \hat{e}_2)} e^{\zeta_2 (\sqrt{1-\eta} \hat{a}_2^{\dagger} - \sqrt{\eta} \hat{e}_2^{\dagger})} \rangle_w$$
(A.8)

$$= \langle e^{-\zeta_1^* \sqrt{1-\eta} \hat{a}_1} e^{\zeta_1} \sqrt{1-\eta} \hat{a}_1^{\dagger} e^{-\zeta_1^* \sqrt{1-\eta} \hat{a}_2} e^{\zeta_2} \sqrt{1-\eta} \hat{a}_2^{\dagger} e^{\zeta_1^* \sqrt{\eta} \hat{e}_1} e^{-\zeta \sqrt{\eta} \hat{e}_1^{\dagger}} e^{\zeta_2^* \sqrt{\eta} \hat{e}_2} e^{-\zeta \sqrt{\eta} \hat{e}_2^{\dagger}} \rangle_w \quad \text{(A.9)}$$

$$=\chi_{A}^{\hat{\rho}_{a}}\left(\sqrt{1-\eta}\zeta_{1}^{*},\sqrt{1-\eta}\zeta_{1},\sqrt{1-\eta}\zeta_{2}^{*},\sqrt{1-\eta}\zeta_{2}^{*},\sqrt{1-\eta}\zeta_{2}\right)\chi_{A}^{\hat{\rho}_{e}}\left(-\sqrt{\eta}\zeta_{1}^{*},-\sqrt{\eta}\zeta_{1},-\sqrt{\eta}\zeta_{2}^{*},-\sqrt{\eta}\zeta_{2}\right)$$
(A.10)

where (A.8) uses $\hat{w} = \sqrt{1 - \eta \hat{a}} - \sqrt{\eta} \hat{e}$, (A.9) uses the fact that bosonic operators acting on different modes commute with each other, and (A.10) separates the characteristic function into characteristic functions for each input mode of Alice $\chi_A^{\hat{\rho}_a}$, and the environment $\chi_A^{\hat{\rho}_e}$. To derive the characteristic function for mode e, note that the multi-mode thermal state $\hat{\rho}_e$ is

separable, and thus

$$\chi_{A}^{\hat{\rho}_{e}}(-\sqrt{\eta}\zeta_{1}^{*},-\sqrt{\eta}\zeta_{1},-\sqrt{\eta}\zeta_{2}^{*},-\sqrt{\eta}\zeta_{2}) = \chi_{A}^{\hat{\rho}_{e}}(-\sqrt{\eta}\zeta_{1}^{*},-\sqrt{\eta}\zeta_{1})\chi_{A}^{\hat{\rho}_{e}}(-\sqrt{\eta}\zeta_{2}^{*},-\sqrt{\eta}\zeta_{2})$$
 (A.11)

The solution for the single mode $\chi_A^{\hat{\rho}_e}$ is well known, giving

$$\chi_A^{\hat{\rho}_e}(\sqrt{\eta}\zeta_1^*, \sqrt{\eta}\zeta_1, \sqrt{\eta}\zeta_2^*, \sqrt{\eta}\zeta_2) = e^{-(1+N)\eta(|\zeta_1|^2 + |\zeta_2|^2)}.$$
 (A.12)

Now, we calculate the characteristic function for $\hat{\rho}_a$:

$$\chi_A^{\hat{\rho}_a} \left(\sqrt{1 - \eta} \zeta_1^*, \sqrt{1 - \eta} \zeta_1, \sqrt{1 - \eta} \zeta_2^*, \sqrt{1 - \eta} \zeta_2 \right) \tag{A.13}$$

$$= \operatorname{tr}(\hat{\rho}_{a} e^{-\zeta_{1}^{*} \sqrt{1 - \eta} \hat{a}_{1}} e^{\zeta_{1} \sqrt{1 - \eta} \hat{a}_{1}^{\dagger}} e^{-\zeta_{2}^{*} \sqrt{1 - \eta} \hat{a}_{2}} e^{\zeta_{2} \sqrt{1 - \eta} \hat{a}_{2}^{\dagger}})$$
(A.14)

$$= e^{-(1-\eta)(|\zeta_1|^2 + |\zeta_2|^2)} \operatorname{tr}(\hat{\rho}_a e^{\zeta_1} \sqrt{1-\eta} \hat{a}_1^{\dagger} e^{-\zeta_1^*} \sqrt{1-\eta} \hat{a}_1 e^{\zeta_2} \sqrt{1-\eta} \hat{a}_2^{\dagger} e^{-\zeta_2^*} \sqrt{1-\eta} \hat{a}_2)$$
(A.15)

$$=e^{-(1-\eta)(|\zeta_1|^2+|\zeta_2|^2)} \tag{A.16}$$

$$\times \sum_{n=0}^{\infty} \sum_{m=0}^{\infty} \left(\langle nm | \left(|\alpha|^2 |01\rangle \langle 01| + \alpha\beta^* |01\rangle \langle 10| + \alpha^*\beta |10\rangle \langle 01| + |\beta|^2 |10\rangle \langle 10| \right) \right)$$

$$\times e^{\zeta_1 \sqrt{1-\eta} \hat{a}_1^{\dagger}} e^{-\zeta_1^* \sqrt{1-\eta} \hat{a}_1} e^{\zeta_2 \sqrt{1-\eta} \hat{a}_2^{\dagger}} e^{-\zeta_2^* \sqrt{1-\eta} \hat{a}_2} |nm\rangle$$
(A.17)

where the first step applies the Baker-Campbell-Hausdorff theorem, followed by expansion of the trace. This further simplifies via

$$\chi_A^{\hat{\rho}a}\left(\sqrt{1-\eta}\zeta_1^*,\sqrt{1-\eta}\zeta_1,\sqrt{1-\eta}\zeta_2^*,\sqrt{1-\eta}\zeta_2\right)$$

$$=e^{-(1-\eta)(|\zeta_1|^2+|\zeta_2|^2)}\left(|\alpha|^2\langle 01|e^{\zeta_1\sqrt{1-\eta}\hat{a}_1^\dagger}e^{-\zeta_1^*\sqrt{1-\eta}\hat{a}_1}e^{\zeta_2\sqrt{1-\eta}\hat{a}_2^\dagger}e^{-\zeta_2^*\sqrt{1-\eta}\hat{a}_2}|01\rangle\right) \quad (A.18a)$$

$$+\alpha\beta^*\langle 10|e^{\zeta_1}\sqrt{1-\eta}\hat{a}_1^{\dagger}e^{-\zeta_1^*}\sqrt{1-\eta}\hat{a}_1e^{\zeta_2}\sqrt{1-\eta}\hat{a}_2^{\dagger}e^{-\zeta_2^*}\sqrt{1-\eta}\hat{a}_2|01\rangle \tag{A.18b}$$

$$+ \alpha^* \beta \langle 01 | e^{\zeta_1} \sqrt{1 - \eta} \hat{a}_1^{\dagger} e^{-\zeta_1^*} \sqrt{1 - \eta} \hat{a}_1 e^{\zeta_2} \sqrt{1 - \eta} \hat{a}_2^{\dagger} e^{-\zeta_2^*} \sqrt{1 - \eta} \hat{a}_2 | 10 \rangle$$
(A.18c)

$$+ |\beta|^{2} \langle 10|e^{\zeta_{1}}\sqrt{1-\eta}\hat{a}_{1}^{\dagger}e^{-\zeta_{1}^{*}}\sqrt{1-\eta}\hat{a}_{1}e^{\zeta_{2}}\sqrt{1-\eta}\hat{a}_{2}^{\dagger}e^{-\zeta_{2}^{*}}\sqrt{1-\eta}\hat{a}_{2}|10\rangle). \tag{A.18d}$$

Expanding the exponentials for mode 1 of (A.18a) gives us

$$e^{-(1-\eta)(|\zeta_1|^2+|\zeta_2|^2)}|\alpha|^2\langle 01|e^{\zeta_1\sqrt{1-\eta}\hat{a}_1^{\dagger}}e^{-\zeta_1^*\sqrt{1-\eta}\hat{a}_1}e^{\zeta_2\sqrt{1-\eta}\hat{a}_2^{\dagger}}e^{-\zeta_2^*\sqrt{1-\eta}\hat{a}_2}|01\rangle \tag{A.19}$$

$$= e^{-(1-\eta)(|\zeta_1|^2 + |\zeta_2|^2)} |\alpha|^2 \langle 01| \left(\sum_{k'=0}^n (\hat{a}_1^{\dagger})^{k'} \frac{(\sqrt{1-\eta}\zeta)^{k'}}{k'!} \right)$$

$$\times \left(\sum_{k=0}^{n} \frac{\left(-\sqrt{1-\eta} \zeta^{*} \right)^{k}}{k!} (\hat{a}_{1})^{k} \right) e^{-\zeta_{2}^{*} \sqrt{1-\eta} \hat{a}_{2}} e^{\zeta_{2} \sqrt{1-\eta} \hat{a}_{2}^{\dagger}} |01\rangle. \tag{A.20}$$

As mode 1 is in the 0 state, every term in the first Taylor series will cancel unless k' and k are equal to 0. Thus, (A.18a) reduces to

$$e^{-(1-\eta)(|\zeta_1|^2+|\zeta_2|^2)}|\alpha|^2\langle 01|e^{-\zeta_2^*\sqrt{1-\eta}\hat{a}_2}e^{\zeta_2\sqrt{1-\eta}\hat{a}_2^\dagger}|01\rangle. \tag{A.21}$$

Taylor expanding the exponentials for mode 2 in (A.21) yields

$$e^{-(1-\eta)(|\zeta_1|^2+|\zeta_2|^2)}|\alpha|^2\langle 01|\left(\sum_{k'=0}^n(\hat{a}_2^{\dagger})^{k'}\frac{(\sqrt{1-\eta}\zeta)^{k'}}{k'!}\right)\left(\sum_{k=0}^n\frac{\left(-\sqrt{1-\eta}\zeta^*\right)^k}{k!}(\hat{a}_2)^k\right)|01\rangle \quad (A.22)$$

$$= e^{-(1-\eta)(|\zeta_1|^2 + |\zeta_2|^2)} |\alpha|^2 \langle 0| \otimes (\langle 1| + (\sqrt{1-\eta}\zeta_2)\langle 0|) |0\rangle \otimes (|1\rangle - \zeta_2^* \sqrt{1-\eta} |0\rangle) \tag{A.23}$$

$$= e^{-(1-\eta)(|\zeta_1|^2 + |\zeta_2|^2)} |\alpha|^2 (1 - (1-\eta)|\zeta_2|^2). \tag{A.24}$$

Equations (A.18b) to (A.18d) follow similarly to give

$$\chi_A^{\hat{\rho}_w}(\zeta_1^*, \zeta_1, \zeta_2^*, \zeta_2) = e^{-(1+\eta N)(|\zeta_1|^2 + |\zeta_2|^2)} |\alpha|^2 (1 - (1-\eta)|\zeta_2|^2)$$
(A.25a)

$$-e^{-(1+\eta N)(|\zeta_1|^2+|\zeta_2|^2)}\alpha\beta^*(1-\eta)\zeta_1\zeta_2^*$$
 (A.25b)

$$-e^{-(1+\eta N)(|\zeta_1|^2+|\zeta_2|^2)}\alpha^*\beta(1-\eta)\zeta_1^*\zeta_2$$
 (A.25c)

+
$$e^{-(1+\eta N)(|\zeta_1|^2+|\zeta_2|^2)}|\beta|^2(1-(1-\eta)|\zeta_1|^2)$$
 (A.25d)

(A.27f)

A generalize two-mode state can be written as

$$\hat{\rho}_w = \sum_{m=0}^{\infty} \sum_{n=0}^{\infty} \sum_{m'=0}^{\infty} \sum_{n'=0}^{\infty} \langle nm | \hat{\rho}_w | n'm' \rangle | nm \rangle \langle n'm' |$$
(A.26)

where $\langle nm|\hat{\rho}_w|n'm'\rangle$ are the density matrix elements. Armed with the characteristic function, we can derive, $\hat{\rho}_w$ via the operator Fourier transform

$$\hat{\rho}_{\hat{w}} = \sum_{m=0}^{\infty} \sum_{n=0}^{\infty} \sum_{m'=0}^{\infty} \sum_{n'=0}^{\infty} \langle nm|$$

$$\left(|\alpha|^{2} \int \frac{d^{2}\zeta_{2}}{\pi} \int \frac{d^{2}\zeta_{1}}{\pi} e^{-(1+\eta N)(|\zeta_{1}|^{2}+|\zeta_{2}|^{2})} (1-(1-\eta)|\zeta_{2}|^{2}) e^{\zeta_{1}\hat{c}_{1}^{\dagger}} e^{-\zeta_{1}^{*}\hat{c}_{1}} e^{\zeta_{2}\hat{c}_{2}^{\dagger}} e^{-\zeta_{2}^{*}\hat{c}_{2}} \right)$$

$$+ \alpha\beta^{*} \int \frac{d^{2}\zeta_{2}}{\pi} \int \frac{d^{2}\zeta_{1}}{\pi} e^{-(1+\eta N)(|\zeta_{1}|^{2}+|\zeta_{2}|^{2})} (-(1-\eta)\zeta_{1}\zeta_{2}^{*}) e^{\zeta_{1}\hat{c}_{1}^{\dagger}} e^{-\zeta_{1}^{*}\hat{c}_{1}} e^{\zeta_{2}\hat{c}_{2}^{\dagger}} e^{-\zeta_{2}^{*}\hat{c}_{2}}$$

$$(A.27c)$$

$$+ \alpha^{*}\beta \int \frac{d^{2}\zeta_{2}}{\pi} \int \frac{d^{2}\zeta_{1}}{\pi} e^{-(1+\eta N)(|\zeta_{1}|^{2}+|\zeta_{2}|^{2})} (-(1-\eta)\zeta_{1}^{*}\zeta_{2}) e^{\zeta_{1}\hat{c}_{1}^{\dagger}} e^{-\zeta_{1}^{*}\hat{c}_{1}} e^{\zeta_{2}\hat{c}_{2}^{\dagger}} e^{-\zeta_{2}^{*}\hat{c}_{2}}$$

$$(A.27d)$$

$$+ |\beta|^{2} \int \frac{d^{2}\zeta_{2}}{\pi} \int \frac{d^{2}\zeta_{1}}{\pi} e^{-(1+\eta N)(|\zeta_{1}|^{2}+|\zeta_{2}|^{2})} (1-(1-\eta)|\zeta_{1}|^{2}) e^{\zeta_{1}\hat{c}_{1}^{\dagger}} e^{-\zeta_{1}^{*}\hat{c}_{1}} e^{\zeta_{2}\hat{c}_{2}^{\dagger}} e^{-\zeta_{2}^{*}\hat{c}_{2}}$$

$$(A.27d)$$

$$+ |\beta|^{2} \int \frac{d^{2}\zeta_{2}}{\pi} \int \frac{d^{2}\zeta_{1}}{\pi} e^{-(1+\eta N)(|\zeta_{1}|^{2}+|\zeta_{2}|^{2})} (1-(1-\eta)|\zeta_{1}|^{2}) e^{\zeta_{1}\hat{c}_{1}^{\dagger}} e^{-\zeta_{1}^{*}\hat{c}_{1}} e^{\zeta_{2}\hat{c}_{2}^{\dagger}} e^{-\zeta_{2}^{*}\hat{c}_{2}}$$

$$(A.27e)$$

$$|n'm'\rangle |nm\rangle\langle n'm'|$$

The integrals are separable with respect to each mode, simplifying to

$$\begin{split} \hat{\rho}_{\hat{w}} &= \sum_{m=0}^{\infty} \sum_{n=0}^{\infty} \sum_{m'=0}^{\infty} \sum_{n'=0}^{\infty} \langle nm | \\ & \left(|\alpha|^2 \frac{d^2 \zeta_2}{\pi} e^{-(1+\eta N)|\zeta_2|^2} (1-(1-\eta)|\zeta_2|^2) e^{\zeta_2 \hat{c}_2^{\dagger}} e^{-\zeta_2^* \hat{c}_2} \int \frac{d^2 \zeta_1}{\pi} e^{-(1+\eta N)|\zeta_1|^2} e^{\zeta_1 \hat{c}_1^{\dagger}} e^{-\zeta_1^* \hat{c}_1} \\ & (A.28a) \\ & -\alpha \beta^* (1-\eta) \int \frac{d^2 \zeta_2}{\pi} e^{-(1+\eta N)|\zeta_2|^2} \zeta_2^* e^{\zeta_2 \hat{c}_2^{\dagger}} e^{-\zeta_2^* \hat{c}_2} \int \frac{d^2 \zeta_1}{\pi} \zeta_1 e^{-(1+\eta N)|\zeta_1|^2} e^{\zeta_1 \hat{c}_1^{\dagger}} e^{-\zeta_1^* \hat{c}_1} \\ & (A.28b) \\ & -\alpha^* \beta (1-\eta) \int \frac{d^2 \zeta_2}{\pi} e^{-(1+\eta N)|\zeta_2|^2} \zeta_2 e^{\zeta_2 \hat{c}_2^{\dagger}} e^{-\zeta_2^* \hat{c}_2} \int \frac{d^2 \zeta_1}{\pi} \zeta_1^* e^{-(1+\eta N)|\zeta_1|^2} e^{\zeta_1 \hat{c}_1^{\dagger}} e^{-\zeta_1^* \hat{c}_1} \\ & (A.28c) \\ & + |\beta|^2 \int \frac{d^2 \zeta_2}{\pi} e^{-(1+\eta N)|\zeta_2|^2} e^{\zeta_2 \hat{c}_2^{\dagger}} e^{-\zeta_2^* \hat{c}_2} \int \frac{d^2 \zeta_1}{\pi} e^{-(1+\eta N)|\zeta_1|^2} (1-(1-\eta)|\zeta_1|^2) e^{\zeta_1 \hat{c}_1^{\dagger}} e^{-\zeta_1^* \hat{c}_1} \\ & (A.28d) \\ & |n'm'\rangle |nm\rangle \langle n'm'| \end{split}$$

Next, we calculate $\langle nm|\hat{\rho}_w|n'm'\rangle$ for each term in Equations (A.28a) to (A.28d). We first convert to polar coordinates, and utilize Lemma C.1 to solve the integral over θ . (A.28a) simplifies to

$$4|\alpha|^2 \int_{r_2=0}^{\infty} dr_2 r_2 (1 - (1 - \eta)r_2^2) e^{-(1 + \eta N)r_2^2} \mathcal{L}_m(r_2^2) \int_{r_1=0}^{\infty} dr_1 r_1 e^{-(1 + \eta N)r_1^2} \mathcal{L}_n(r_1^2)$$
 (A.29)

These integrals further are evaluated via:

$$|\alpha|^2 \frac{(\eta N)^n}{(1+\eta N)^{n+1}} \left(\frac{(\eta N)^m}{(1+\eta N)^{m+1}} - \frac{(1-\eta)(\eta N-m)(\eta N)^{m-1}}{(1+\eta N)^{m+2}} \right). \tag{A.30}$$

Likewise, the integrals in (A.28d) is exactly the same with m and n swapped:

$$|\beta|^2 \frac{(\eta N)^m}{(1+\eta N)^{m+1}} \left(\frac{(\eta N)^n}{(1+\eta N)^{n+1}} - \frac{(1-\eta)(\eta N - n)(\eta N)^{n-1}}{(1+\eta N)^{n+2}} \right). \tag{A.31}$$

For the integrals in (A.28b) we follow the same procedure, where we first convert to polar

coordinates and use Lemma C.2 to solve the integral over θ . This produces

$$-\alpha\beta^{*}(1-\eta)\left(\int \frac{d^{2}\zeta_{2}}{\pi}e^{-(1+\eta N)|\zeta_{2}|^{2}}\zeta_{2}^{*}e^{\zeta_{2}\hat{c}_{2}^{\dagger}}e^{-\zeta_{2}^{*}\hat{c}_{2}}\right)\left(\int \frac{d^{2}\zeta_{1}}{\pi}\zeta_{1}e^{-(1+\eta N)|\zeta_{1}|^{2}}e^{\zeta_{1}\hat{c}_{1}^{\dagger}}e^{-\zeta_{1}^{*}\hat{c}_{1}}\right)$$
(A.32)

$$= -4\alpha\beta^*(1-\eta)\sqrt{m+1}\sqrt{n'+1}\int_{r_2=0}^{\infty}dr_2r_2^3e^{-(1+\eta N)r_2^2}\sum_{k=0}^{m}(r_2^2)^k\frac{(-1)^k}{k!}\binom{m}{k}\frac{1}{k+1}$$

$$\times \int_{r_1=0}^{\infty} dr_1 r_1^3 e^{-(1+\eta N)r_1^2} \sum_{l=0}^{n'} (r_1^2)^l \frac{(-1)^l}{l!} \binom{n'}{l} \frac{1}{l+1}$$
(A.33)

$$= -\alpha \beta^* (1-\eta) \sqrt{m+1} \sqrt{n'+1} \sum_{k=0}^m \frac{(k+1)!}{(1+\eta N)^{k+2}} \frac{(-1)^k}{k!} \binom{m}{k} \frac{1}{k+1}$$

$$\times \sum_{l=0}^{n'} \frac{(l+1)!}{(1+\eta N)^{l+2}} \frac{(-1)^l}{l!} \binom{n'}{l} \frac{1}{l+1}$$
(A.34)

$$= -\alpha \beta^* (1 - \eta) \sqrt{m + 1} \sqrt{n' + 1} \sum_{k=0}^{m} \frac{(-1)^k}{(1 + \eta N)^{k+2}} \binom{m}{k} \sum_{l=0}^{n'} \frac{(-1)^l}{(1 + \eta N)^{l+2}} \binom{n'}{l}$$
(A.35)

$$= -\alpha \beta^* (1 - \eta) \sqrt{m + 1} \sqrt{n' + 1} \frac{(\eta N)^m}{(1 + \eta N)^{m+2}} \frac{(\eta N)^{n'}}{(1 + \eta N)^{n'+2}}$$
(A.36)

$$= -\alpha \beta^* (1 - \eta) \sqrt{m+1} \sqrt{n} \frac{(\eta N)^{m+n-1}}{(1 + \eta N)^{m+n+3}}$$
(A.37)

Finally, in (A.37) we convert n' + 1 to n, which is a consequence of the $\delta_{n,n'+1}$ term in Lemma C.2. The integrals in (A.28c) follow the exact same steps to yield

$$-\alpha^{*}\beta(1-\eta)\left(\int \frac{d^{2}\zeta_{2}}{\pi}e^{-(1+\eta N)|\zeta_{2}|^{2}}\zeta_{2}e^{\zeta_{2}\hat{c}_{2}^{\dagger}}e^{-\zeta_{2}^{*}\hat{c}_{2}}\right)\left(\int \frac{d^{2}\zeta_{1}}{\pi}\zeta_{1}^{*}e^{-(1+\eta N)|\zeta_{1}|^{2}}e^{\zeta_{1}\hat{c}_{1}^{\dagger}}e^{-\zeta_{1}^{*}\hat{c}_{1}}\right)$$
(A.38)

$$= -\alpha^* \beta (1 - \eta) \sqrt{m} \sqrt{n+1} \frac{(\eta N)^{m+n-1}}{(1 + \eta N)^{m+n+3}}.$$
(A.39)

Replacing the $\langle nm|\hat{\rho}_w|n'm'\rangle$ term in (A.26) with eqs. (A.30), (A.31), (A.37) and (A.39) yields

$$\begin{split} \hat{\rho}_{w} &= \sum_{m=0}^{\infty} \sum_{n=0}^{\infty} \left(|\alpha|^{2} \frac{(\eta N)^{n}}{(1+\eta N)^{n+1}} \left(\frac{(\eta N)^{m}}{(1+\eta N)^{m+1}} - \frac{(1-\eta)(\eta N-m)(\eta N)^{m-1}}{(1+\eta N)^{m+2}} \right) \right. \\ &+ |\beta|^{2} \frac{(\eta N)^{m}}{(1+\eta N)^{m+1}} \left(\frac{(\eta N)^{n}}{(1+\eta N)^{n+1}} - \frac{(1-\eta)(\eta N-n)(\eta N)^{n-1}}{(1+\eta N)^{n+2}} \right) \right) |nm\rangle\langle nm| \\ &- \alpha^{*}\beta(1-\eta)\sqrt{m}\sqrt{n+1} \frac{(\eta N)^{m+n-1}}{(1+\eta N)^{m+n+3}} |nm\rangle\langle n+1, m-1| \\ &- \alpha\beta^{*}(1-\eta)\sqrt{m+1}\sqrt{n} \frac{(\eta N)^{m+n-1}}{(1+\eta N)^{m+n+3}} |nm\rangle\langle n-1, m+1| \end{split} \tag{A.40}$$

where the $\langle n+1, m-1 |$ and $\langle n-1, m+1 |$ terms arise from the off-by-one integrals over θ as per Lemma C.2.

A.2. Calculating the χ^2 -divergence

The χ^2 -divergence we are after is $D_{\chi^2}(\hat{\rho}^W_{\alpha,\beta}||\hat{\rho}^W_0)$ where $\hat{\rho}^W_0$ is defined in (A.1) and $\hat{\rho}^W_{\alpha,\beta}$ is exactly $\hat{\rho}_w$ from (A.40). We note that

$$D_{\chi^2}(\hat{\rho}_{\alpha,\beta}^W||\hat{\rho}_0^W) = \text{Tr}[(\hat{\rho}_{\alpha,\beta}^W - \hat{\rho}_0^W)^2 \hat{\rho}_b^{-1}]$$
(A.41)

$$= \text{Tr}[(\hat{\rho}_{\alpha,\beta}^{W})^{2}(\hat{\rho}_{0}^{W})^{-1}] - 1. \tag{A.42}$$

Due to $\hat{\rho}_0^W$ being diagonal, $(\hat{\rho}_0^W)^{-1}$ is also diagonal and involves calculating the reciprocal of the elements. Consequently, only the diagonal elements of $(\hat{\rho}_{\alpha,\beta}^W)^2$ are required to evaluate $(\hat{\rho}_{\alpha,\beta}^W)^2(\hat{\rho}_0^W)^{-1}$. As $\hat{\rho}_{\alpha,\beta}^W$ is a tri-diagonal state, we can decompose it into three matrices A,B, and D where each of the individual matrices correspond to one of the diagonals. Then we write $\hat{\rho}_{\alpha,B}^W = A + B + D$ where

$$D = \sum_{n=0}^{\infty} \sum_{m=0}^{\infty} d_{nm} |nm\rangle \langle nm|$$
(A.43)

$$A = \sum_{n=0}^{\infty} \sum_{m=1}^{\infty} a_{nm} |nm\rangle \langle n+1, m-1|$$
 (A.44)

$$B = \sum_{n=1}^{\infty} \sum_{m=0}^{\infty} b_{nm} |nm\rangle \langle n-1, m+1|,$$
 (A.45)

and the coefficients are given by

$$d_{nm} = |\alpha|^2 \frac{(\eta N)^n}{(1+\eta N)^{n+1}} \left(\frac{(\eta N)^m}{(1+\eta N)^{m+1}} - \frac{(1-\eta)(\eta N-m)(\eta N)^{m-1}}{(1+\eta N)^{m+2}} \right) + |\beta|^2 \frac{(\eta N)^m}{(1+\eta N)^{m+1}} \left(\frac{(\eta N)^n}{(1+\eta N)^{n+1}} - \frac{(1-\eta)(\eta N-n)(\eta N)^{n-1}}{(1+\eta N)^{n+2}} \right)$$

$$(A.46)$$

$$a_{nm} = -\alpha^* \beta (1 - \eta) \sqrt{m} \sqrt{n + 1} \frac{(\eta N)^{m+n-1}}{(1 + \eta N)^{m+n+3}}$$
(A.47)

$$b_{nm} = -\alpha \beta^* (1 - \eta) \sqrt{m + 1} \sqrt{n} \frac{(\eta N)^{m+n-1}}{(1 + \eta N)^{m+n+3}}$$
(A.48)

We then expand $(\hat{\rho}_{\alpha,\beta}^W)^2$ as

$$(\hat{\rho}_{\alpha,\beta}^W)^2 = (A + B + D)^2$$
 (A.49)

$$= A^{2} + AB + AD + BA + B^{2} + BD + DA + DB + D^{2}$$
(A.50)

Each of the terms evaluate as follows via replacement from Equations (A.43) to (A.45) and

orthonomality of the Fock states,

$$A^{2} = \sum_{n=0}^{\infty} \sum_{m=2}^{\infty} a_{nm} a_{n+1,m-1} |nm\rangle \langle n+2, m-2|$$
 (A.51)

$$B^{2} = \sum_{n=2}^{\infty} \sum_{m=0}^{\infty} b_{nm} b_{n-1,m+1} |nm\rangle \langle n-2, m+2|$$
(A.52)

$$D^{2} = \sum_{n=0}^{\infty} \sum_{m=0}^{\infty} d_{nm}^{2} |nm\rangle\langle nm|$$
(A.53)

$$AB = \sum_{n=0}^{\infty} \sum_{m=1}^{\infty} a_{nm} b_{n+1,m-1} |nm\rangle \langle nm|$$
(A.54)

$$BA = \sum_{n=1}^{\infty} \sum_{m=0}^{\infty} a_{n-1,m+1} b_{nm} |nm\rangle \langle nm|$$
(A.55)

$$AD = DA = \sum_{n=0}^{\infty} \sum_{m=1}^{\infty} a_{nm} d_{n+1,m-1} |nm\rangle \langle n+1, m-1|$$
 (A.56)

$$BD = DB = \sum_{n=1}^{\infty} \sum_{m=0}^{\infty} b_{nm} d_{n-1,m+1} |nm\rangle \langle n-1, m+1|.$$
 (A.57)

Hence, the only terms that contribute to the main diagonal of $(\hat{\rho}_{\alpha,\beta}^W)^2$ are D^2 , AB, and BA. Thus

$$D_{\chi^2}(\hat{\rho}_{\alpha,\beta}^W||\hat{\rho}_0^W) = \text{Tr}[(\hat{\rho}_{\alpha,\beta}^W)^2(\hat{\rho}_0^W)^{-1}] - 1 \tag{A.58}$$

$$= -1 + \sum_{n=0,m=0}^{\infty} (d_{nm}^2 + a_{nm}b_{n+1,m-1} + a_{n-1,m+1}b_{nm})t_{nm}^{-1}$$
(A.59)

$$= -1 + \frac{(|\alpha|^4 + |\beta|^4)(1 + \eta(-2 + \eta + N + \eta N^2))}{\eta N(1 + \eta N)} + 2|\alpha|^2|\beta|^2 - \frac{2|\alpha|^2|\beta|^2(1 - \eta)^2}{\eta N(1 + \eta N)}$$
(A.60)

$$=\frac{(1-\eta)^2}{\eta N(1+\eta N)} \tag{A.61}$$

where t_{nm}^{-1} are the inverse diagonal elements of the thermal state in (A.1). The full expansion of the terms is omitted here for space consideration, yet they simplify to (A.60) using standard grade-school algebra and known closed forms of the summations. Furthermore, we utilize the constraint that $|\alpha|^2 + |\beta|^2 = (|\alpha|^2 + |\beta|^2)^2 = 1$ to arrive at (A.61) completing the proof.

Appendix B. Induced Entanglement Breaking Channel

B.1. Proof of Lemma 1

Alice utilizes the system devised in Fig. 2 where she inputs her qubit state to a beamsplitter with transmissivity τ . The output of the beamsplitter is passed through the channel modeled by a second beamsplitter with transmissivity η . Alice has control over τ and it's second input state at the mode labeled \hat{e} . The input-output modal relationships of the system are

$$\hat{a}' = \sqrt{\tau}\hat{a} + \sqrt{1 - \tau}\hat{u} \tag{B.1}$$

$$\hat{w} = \sqrt{1 - \eta} \hat{a}' - \sqrt{\eta} \hat{e} \tag{B.2}$$

$$\hat{w} = \sqrt{\tau(1-\eta)}\hat{a} + \sqrt{(1-\tau)(1-\eta)}\hat{u} - \sqrt{\eta}\hat{e}$$
 (B.3)

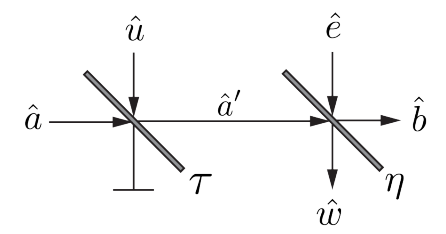


Fig. 2. A system Alice can employ to induce an entanglement breaking channel. Annihilation operators \hat{a} , \hat{u} and \hat{e} label Alice's and the environment's input modes, while \hat{w} and \hat{b} label Bob's and warden Willie's output modes. \hat{a}' labels an intermediate mode that is the output of the first beamsplitter with transmissivity τ and input into the beamsplitter with transmissivity η . Alice has control over the beamsplitter transmissivity τ and the input state at the mode labeled \hat{u} . The beamsplitter with transmissivity η and input state at \hat{e} represent the original system channel in Fig. 1 and are fixed.

To demonstrate the state at Willie is equivalent to the original channel with adjusted transmissivity and additional noise, we can utilize the characteristic functions of the system. Additionally, without lack of generality, we consider the single-mode case, therefore we need to show

$$\chi_A^{\hat{\rho}_W}(\zeta^*, \zeta) = \chi_A^{\hat{\rho}_a} \left(\sqrt{\tau (1 - \eta)} \zeta^*, \sqrt{\tau (1 - \eta)} \zeta \right) e^{-(1 + \eta (N + N'))|\zeta|^2}$$
(B.4)

where N is the thermal mean photon number of the environment state and N' is the additional thermal mean photon number Alice introduces. The exponential is of the same form as the single mode version of (A.12). It follows then

$$\chi_A^{\hat{\rho}_W}(\zeta^*, \zeta) = \chi_A^{\hat{\rho}_a} \left(\sqrt{\tau (1 - \eta)} \zeta^*, \sqrt{\tau (1 - \eta)} \zeta \right)$$

$$\times \chi_A^{\hat{\rho}_u} \left(\sqrt{(1 - \tau)(1 - \eta)} \zeta^*, \sqrt{(1 - \tau)(1 - \eta)} \zeta \right) \chi_A^{\hat{\rho}_e} \left(\sqrt{\eta} \zeta^*, \sqrt{\eta} \zeta \right)$$
(B.5)

$$=\chi_A^{\hat{\rho}_a}\left(\sqrt{\tau(1-\eta)}\zeta^*,\sqrt{\tau(1-\eta)}\zeta\right)e^{-(1-\tau)(1-\eta)|\zeta|^2}e^{-(1+N)\eta|\zeta|^2} \tag{B.6}$$

$$= \chi_A^{\hat{\rho}_a} \left(\sqrt{\tau (1 - \eta)} \zeta^*, \sqrt{\tau (1 - \eta)} \zeta \right) e^{-(1 + N + \frac{(1 - \tau)(1 - \eta)}{\eta}) \eta |\zeta|^2}$$
(B.7)

$$= \chi_A^{\hat{\rho}_a} \left(\sqrt{\tau (1 - \eta)} \zeta^*, \sqrt{\tau (1 - \eta)} \zeta \right) e^{-(1 + N + N') \eta |\zeta|^2}$$
(B.8)

As the inputs to the system are not entangled with each other, in (B.5) we split the characteristic function into the components of the inputs following (B.3). In (B.6), the characteristic functions are evaluated for input states of vacuum and a 0-mean thermal state with thermal mean photon number N at the modes labeled \hat{u} and \hat{e} respectively. The form of (B.8) matches that of a single-mode input state to the original channel (see eqs. (A.10) and (A.12)) with signal transmissivity of $\tau(1-\eta)$ and mean thermal-noise photons of $\eta N + \eta N' = \eta N + (1-\tau)(1-\eta)$. Substituting these in the entanglement breaking constraint for the original channel yields a new constraint of $\eta N > (1-\eta)(1-2\tau)$ which completes the proof.

B.2. Proof of Lemma 2

Alice utilizes the system devised in Fig. 3 where she inputs her qubit state to a quantum-limited amplifier with gain coefficient G. The output of the amplifier is then fed to a beamsplitter of transmissivity τ . Finally the signal is passed through the channel modeled by a beamsplitter with transmissivity η . Alice has control over G, τ , and the second input states to the amplifier and beamsplitter with transmissivity τ . η and the environment input state at the mode labeled \hat{e} are

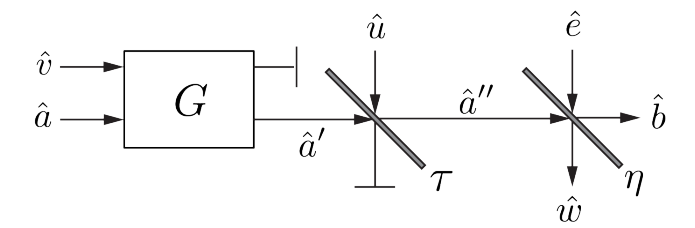


Fig. 3. A system that allows Alice to introduce additional arbitrary thermal noise in the Alice-to-Willie channel. Annihilation operators \hat{a} and \hat{v} Alice's input into the quantum-limited amplifier with gain coefficient G. The output of the amplifier is labeled by annihilation operator \hat{a}' and is input to a beamsplitter with transmissivity τ . The other port for the beamsplitter is labeled with \hat{u} . One output mode of the beamsplitter is traced out, while the other is labeled \hat{a}'' and is the input to a beamsplitter with transmissivity η with a second input mode labeled \hat{e} . The mode labeled \hat{e} and beamsplitter with transmissivity η represent the original system channel in Fig. 1 and are fixed. Alice has control of G, τ , and the input states at modes \hat{v} and \hat{u} with her original qubit state input at \hat{a} .

fixed. The input-output modal relationships of the system are

$$\hat{a}' = \sqrt{G}\hat{a} + \sqrt{G - 1}\hat{v} \tag{B.9}$$

$$\hat{a}^{\prime\prime} = \sqrt{\tau}\hat{a}^{\prime} + \sqrt{1 - \tau}\hat{u} \tag{B.10}$$

$$\hat{w} = \sqrt{1 - \eta} \hat{a}^{"} - \sqrt{\eta} \hat{e} \tag{B.11}$$

$$\hat{w} = \sqrt{\tau (1 - \eta)} \hat{a}' + \sqrt{(1 - \tau)(1 - \eta)} \hat{u} - \sqrt{\eta} \hat{e}$$
(B.12)

$$\hat{w} = \sqrt{G\tau(1-\eta)}\hat{a} + \sqrt{(G-1)\tau(1-\eta)}\hat{v} + \sqrt{(1-\tau)(1-\eta)}\hat{u} - \sqrt{\eta}\hat{e}$$
 (B.13)

To demonstrate the state at Willie is equivalent to the original channel with additional noise, we utilize the characteristic functions of the system. Additionally, without lack of generality, we consider the single-mode case, therefore we need to show

$$\chi_A^{\hat{\rho}_w}(\zeta^*, \zeta) = \chi_A^{\hat{\rho}_a} \left(\sqrt{1 - \eta} \zeta^*, \sqrt{1 - \eta} \zeta \right) e^{-(1 + \eta(N + N'))|\zeta|^2}$$
(B.14)

where N is the thermal mean photon number of the environment state and N' is the additional thermal mean photon number Alice introduces. The exponential is of the same form as the single

mode version of (A.12). It follows then that

$$\begin{split} \chi_{A}^{\hat{\rho}_{w}}\left(\zeta^{*},\zeta\right) &= \chi_{A}^{\hat{\rho}_{a}}\left(\sqrt{G\tau(1-\eta)}\zeta^{*},\sqrt{G\tau(1-\eta)}\zeta\right) \\ &\times \chi_{A}^{\hat{\rho}_{v}}\left(\sqrt{(G-1)\tau(1-\eta)}\zeta^{*},\sqrt{(G-1)\tau(1-\eta)}\zeta\right) \\ &\times \chi_{A}^{\hat{\rho}_{u}}\left(\sqrt{(1-\tau)(1-\eta)}\zeta^{*},\sqrt{(1-\tau)(1-\eta)}\zeta\right)\chi_{A}^{\hat{\rho}_{e}}\left(\sqrt{\eta}\zeta^{*},\sqrt{\eta}\zeta\right) \\ &= \chi_{A}^{\hat{\rho}_{a}}\left(\sqrt{1-\eta}\zeta^{*},\sqrt{1-\eta}\zeta\right)\chi_{A}^{\hat{\rho}_{v}}\left(\sqrt{(1-\frac{1}{G})(1-\eta)}\zeta^{*},\sqrt{(1-\frac{1}{G})(1-\eta)}\zeta\right) \\ &\times \chi_{A}^{\hat{\rho}_{u}}\left(\sqrt{(1-\frac{1}{G})(1-\eta)}\zeta^{*},\sqrt{(1-\frac{1}{G})(1-\eta)}\zeta\right)\chi_{A}^{\hat{\rho}_{e}}\left(\sqrt{\eta}\zeta^{*},\sqrt{\eta}\zeta\right) \\ &= \chi_{A}^{\hat{\rho}_{a}}\left(\sqrt{1-\eta}\zeta^{*},\sqrt{1-\eta}\zeta\right)e^{-(1-\frac{1}{G})(1-\eta)|\zeta|^{2}}e^{-(1-\frac{1}{G})(1-\eta)|\zeta|^{2}}e^{-(1+N)\eta|\zeta|^{2}} \\ &= \chi_{A}^{\hat{\rho}_{a}}\left(\sqrt{1-\eta}\zeta^{*},\sqrt{1-\eta}\zeta\right)e^{-(1+\eta(N+\frac{2}{\eta}(1-\eta)(1-\frac{1}{G}))|\zeta|^{2}} \\ &= \chi_{A}^{\hat{\rho}_{a}}\left(\sqrt{1-\eta}\zeta^{*},\sqrt{1-\eta}\zeta\right)e^{-(1+(N+N'))\eta)|\zeta|^{2}}. \end{split} \tag{B.18} \\ &= \chi_{A}^{\hat{\rho}_{a}}\left(\sqrt{1-\eta}\zeta^{*},\sqrt{1-\eta}\zeta\right)e^{-(1+(N+N'))\eta)|\zeta|^{2}}. \end{split}$$

As the inputs to the system are not entangled with each other, in (B.15) we split the characteristic function into the components of the inputs following (B.13). In (B.16), we set $\tau = 1/G$, and in (B.17) we evaluate $\chi_A^{\hat{\rho}_v}$, $\chi_A^{\hat{\rho}_u}$, and $\chi_A^{\hat{\rho}_e}$ for respective input states of $\hat{\rho}_v = \hat{\rho}_u = |0\rangle\langle 0|$ and $\hat{\rho}_e$ is a 0-mean thermal state with thermal mean photon number N. In (B.18) and (B.19) we show that the characteristic function of Willie's state is equivalent to that of our original channel with additional thermal noise $N' = \frac{2}{\eta}(1-\eta)(1-\frac{1}{G})$. Solving for G yields $G = (2(1-\eta)/(2(1-\eta)-\eta N'))$ completing the proof.

Appendix C. Useful Lemmas

Lemma C.1.

$$\int_{\theta=0}^{2\pi} d\theta \langle m | e^{r(\cos(\theta)+i\sin(\theta))\hat{c}^{\dagger}} e^{-r(\cos(\theta)-i\sin(\theta))\hat{c}} | m' \rangle = 2\pi \mathcal{L}_m(r^2)$$
 (C.1)

Proof.

$$\int_{\theta=0}^{2\pi} d\theta \langle m|e^{r(\cos(\theta)+i\sin(\theta))\hat{c}^{\dagger}}e^{-r(\cos(\theta)-i\sin(\theta))\hat{c}}|m'\rangle \qquad (C.2)$$

$$= \int_{\theta=0}^{2\pi} d\theta \left(\sum_{k'=0}^{\infty} \langle m|\frac{r^{k'}(\cos(\theta)+i\sin(\theta))^{k'}}{k'!}(\hat{c}^{\dagger})^{k'}\right) \left(\sum_{k=0}^{\infty} \frac{(-r)^k(\cos(\theta)-i\sin(\theta))^k}{k!}\hat{c}^k|m\rangle\right) \qquad (C.3)$$

$$= \sum_{k'=0}^{\infty} \sum_{k=0}^{\infty} \langle m | 2\pi \delta_{k,k'} \frac{r^{k'}}{k'!} (\hat{c}^{\dagger})^{k'} \frac{(-r)^k}{k!} \hat{c}^k | m' \rangle$$
 (C.4)

$$=2\pi \sum_{k=0}^{m} \frac{(-r^2)^k}{k!} \sqrt{\frac{1}{k!^2} \frac{m!}{(m-k)!} \frac{m'!}{(m'-k)!}} \langle m-k|m'-k\rangle$$
 (C.5)

$$=2\pi\sum_{k=0}^{m}\frac{(-r^2)^k}{k!}\sqrt{\binom{m}{k}\binom{m'}{k}}\delta_{m,m'}$$
(C.6)

$$=2\pi \sum_{k=0}^{m} \frac{(-r^2)^k}{k!} \binom{m}{k}$$
 (C.7)

$$=2\pi\mathcal{L}_m(r^2)\tag{C.8}$$

In (C.3), we Taylor expand the exponential terms, followed by evaluating the integral over θ in (C.4) which gives $2\pi\delta_{k,k'}$ allowing us to sum over a single k from k=0 to k=m in (C.5). Furthermore in (C.5), we apply the $(\hat{c}^{\dagger})^k$ and \hat{c}^k operators to their respective bra and ket. In (C.6), the $\delta_{m,m'}$ allows for setting m'=m to simplify to (C.7). Finally, the summation is equivalent to the Laguerre polynomial $\mathcal{L}_m(r^2)$ in (C.8).

Lemma C.2.

$$\int_{\theta=0}^{2\pi} d\theta (\cos(\theta) - i\sin(\theta)) \langle m|e^{r(\cos(\theta) + i\sin(\theta))\hat{c}^{\dagger}} e^{-r(\cos(\theta) - i\sin(\theta))\hat{c}} |m'\rangle$$

$$= -2\pi r \sqrt{m} \sum_{k'=0}^{m+1} (r^2)^{k'} \frac{(-1)^{k'}}{k'!} \binom{m}{k'} \frac{1}{k'+1}$$
(C.9)

Proof.

$$\int_{\theta=0}^{2\pi} d\theta (\cos(\theta) - i\sin(\theta)) \langle m|e^{r(\cos(\theta) + i\sin(\theta))\hat{c}^{\dagger}}e^{-r(\cos(\theta) - i\sin(\theta))\hat{c}}|m'\rangle$$
 (C.10)

$$= \int_{\theta=0}^{2\pi} d\theta \left(\sum_{k'=0}^{\infty} \langle m | \frac{r^{k'} (\cos(\theta) + i\sin(\theta))^{k'}}{k'!} (\hat{c}^{\dagger})^{k'} \right) \left(\sum_{k=0}^{\infty} \frac{(-r)^k (\cos(\theta) - i\sin(\theta))^{k+1}}{k!} \hat{c}^k | m \rangle \right) \tag{C.11}$$

$$= \sum_{k'=0}^{\infty} \sum_{k=0}^{\infty} \langle m | 2\pi \delta_{k+1,k'} \frac{r^{k'}}{k'!} (\hat{c}^{\dagger})^{k'} \frac{(-r)^k}{k!} \hat{c}^k | m' \rangle$$
 (C.12)

$$=2\pi\sum_{k=0}^{\infty}\frac{r(-r^2)^k}{(k+1)!}\sqrt{\frac{1}{k!^2}\frac{m!}{(m-k-1)!}\frac{m'!}{(m'-k)!}}\langle m-k-1|m'-k\rangle \tag{C.13}$$

$$=2\pi r \sum_{k=0}^{m'+1} \frac{(-r^2)^k}{(k+1)k!} \sqrt{\frac{m!}{k!(m-k-1)!} \frac{m'!}{k!(m'-k)!}} \delta_{m,m'+1}$$
(C.14)

$$=2\pi r \sum_{k=0}^{m'+1} \frac{(-r^2)^k}{(k+1)k!} \sqrt{\frac{(m'+1)m'!}{k!(m'-k)!}} \frac{m'!}{k!(m'-k)!}$$
(C.15)

$$=2\pi r\sqrt{m'+1}\sum_{k'=0}^{m'}(r^2)^{k'}\frac{(-1)^{k'}}{k'!}\binom{m'}{k'}\frac{1}{k'+1}$$
(C.16)

(C.17)

The proof follows the same as that of Lemma C.1 except for the off-by-one $\delta_{m,m'+1}$ in (C.14) which we utilize over $\delta_{m-1,m'}$ as $m \in \mathbb{N}_0$. In the final step, we truncate the summation to m' as opposed to m'+1 as the m'+1 term is 0.